Tetrahedron Letters 50 (2009) 1828–1833

Contents lists available at ScienceDirect

Tetrahedron Letters

journal homepage: www.elsevier.com/locate/tetlet

Regioselective N-alkylation of imidazo[4,5-*b*]pyridine-4-oxide derivatives: an experimental and DFT study

Wael Zeinyeh [a], Julien Pilmé [b,c,*], Sylvie Radix [a,*], Nadia Walchshofer [a]

[a] Université de Lyon, Université Lyon 1, ISPB-Faculté de Pharmacie, INSERM U863, IFR 62, F-69373 Lyon cedex 08, France
[b] Université de Lyon, Université Lyon 1, ISPB-Faculté de Pharmacie, F-69373 Lyon cedex 08, France
[c] Laboratoire de Chimie Théorique, Université Pierre et Marie Curie, Paris VI, UMR-CNRS 7616, 4 Place Jussieu, 75252, Paris cedex, France

ARTICLE INFO

Article history:
Received 15 December 2008
Revised 29 January 2009
Accepted 3 February 2009
Available online 8 February 2009

Keywords:
N-alkylation
DFT calculations
Imidazo[4,5-*b*]pyridine
Regioselectivity
S_N2 mechanism
Tautomerism

ABSTRACT

Regioselectivities were determined for N-alkylations of imidazo[4,5-*b*]pyridine-4-oxide and 2-methyl-imidazo[4,5-*b*]pyridine-4-oxide with benzyl bromide or benzyl iodide at RT using K_2CO_3 in DMF as a base. Experimental attempts have shown that *N*-1/*N*-3 ratios slightly varied according to the substitution on *C*-2 position. This was confirmed by DFT calculations in solvent phase. This computational study has shown first that this N-benzylation reaction passed through a S_N2 mechanism. Moreover, regioselectivity of N-benzylation has appeared essentially governed by 'steric approach control'. It explained that opposite *N*-1/*N*-3 ratios were obtained with imidazo[4,5-*b*]pyridine-4-oxide and its 2-methyl-substituted analog. Finally, regioselectivities slightly varied with the nature of benzyl halide.

1. Introduction

The multidrug resistance (MDR) phenotype remains a significant impediment to successful chemotherapies used in particular against cancer or parasitic infections. MDR transporters are involved in the efflux of xenobiotics across biological membranes, and among them, ABC (Adenosine triphosphate–Binding Cassette) transporters couple the hydrolysis of ATP to substrate efflux.[1]

These proteins are therefore potential drug targets of great interest.[2] Imidazo[4,5-*b*]pyridine derivatives which are already known to possess versatile biological activity[3] (antiviral, cytostatic, antimicrobial, fungicidal, cardiovascular, antisecretory, and other functions) can be considered as 1-deazapurine analogs. So, we decided to design new synthetic N-substituted imidazo[4,5-*b*]pyridin-7-one derivatives (Fig. 1) which could target the ATP-binding site contained into ABC transporters. Moreover, it has been often proved that enhancing the selectivity of ATP-binding inhibitors could be achieved via the binding of these inhibitors in neighboring pockets adjacent to the catalytic site.[4] The position and the nature of substituents on imidazopyridinone derivatives are therefore of great importance. So, during the course of our investigations, we decided to study the regioselectivity of N-benzylation of 4-oxide precursors **3** and **4**. Actually, these compounds can exist in two tautomeric forms like benzimidazole or purine systems,[3] and therefore could lead to 1-benzyl- or 3-benzyl-imidazo[4,5-*b*]pyridine-4-oxide **a** or **b** (Fig. 2).

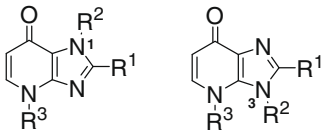

Figure 1. Structures of *N*1- and *N*-3-substituted imidazo[4,5-*b*]pyridin-7-one derivatives.

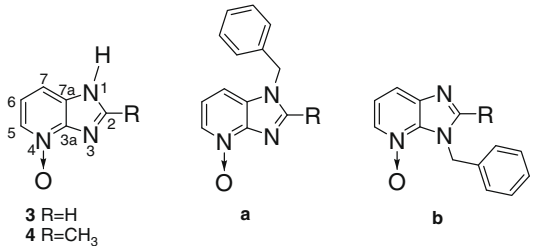

Figure 2. Structures of N-benzylated imidazo[4,5-*b*]pyridine-4-oxide derivatives **a** and **b** and their precursors **3** and **4**.

* Corresponding authors. Tel.: +33 478785609; fax: +33 478785607 (J.P.), tel.: +33 478777253; fax: +33 478777158 (S.R.).
E-mail addresses: julien.pilme@univ-lyon1.fr (J. Pilmé), sylvie.radix@univ-lyon1.fr (S. Radix).

0040-4039/$ - see front matter © 2009 Elsevier Ltd. All rights reserved.
doi:10.1016/j.tetlet.2009.02.006

2. Chemistry

Imidazo[4,5-*b*]pyridine-4-oxide derivatives **3** and **4** were prepared by the two-step sequence that is outlined in Scheme 1. The cyclization to the imidazo[4,5-*b*]pyridine ring system was effected by refluxing the commercially available 2,3-diaminopyridine in triethyl orthoformate or triethyl orthoacetate followed by chlorohydric acid treatment to obtain, respectively, **1**[5] or **2**.[6] The 4-oxide derivatives **3**[7] and **4** were prepared from **1** or **2** according to the Ochiai procedure,[8] namely by oxidation with *meta*-chloroperbenzoic acid in 75% and 79% yield, respectively.[9]

At this point, N-benzylation of imidazopyridine-4-oxides **3** and **4** was carried out under classical conditions of nucleophilic substitution using anhydrous potassium carbonate in DMF solution as a base to generate the corresponding anions **3'** and **4'** (Scheme 2).[10] Whatever the alkylating agent we used (either benzyl bromide or benzyl iodide), the reaction produced a mixture of *N*-1 and *N*-3 regioisomers which were easily separated by flash chromatography.[12] It is worth noting that *N*-1 compounds (**5a** and **6a**) are consistently the more polar ones (silica gel t.l.c.),[11] and have the highest melting point, compared with *N*-3 isomers (**5b** and **6b**).

1D Homonuclear nuclear Overhauser enhancement (nOe) difference spectroscopy was used to establish the structure of each regioisomer synthesized from **3** (**5a** and **5b**). As mentioned in Figure 3, irradiation of the *N*–CH_2 resonance in each regioisomer resulted in nOe effects, respectively, on *C*-7-proton signal for compound **5a** and on *C*-5-proton signal for compound **5b**. Once the regioselectivity of N-benzylation of **3** has been unambiguously determined, it appeared that comparison of ^{1}H NMR spectra allowed to assign easily the structure of *N*-1 and *N*-3 regioisomers (Table 1). Indeed, *C*-7 and *N*–CH_2 proton signals of *N*-1 products (**5a** and **6a**) were significantly shielded compared with the corresponding protons in *N*-3 compounds (**5b** and **6b**): $\Delta\delta = -0.72$ or -0.49 (C^7–H), -0.18 or -0.14 (*N*–CH_2).

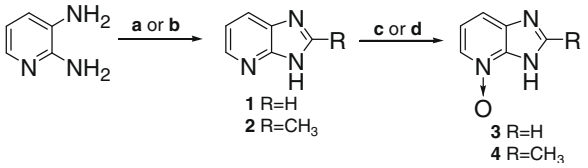

Scheme 1. Reagents and conditions: (a) (i) $HC(OEt)_3$, reflux, 3 h 30 (ii) HCl 37%, reflux, 1 h (83%); (b) (i) $MeC(OEt)_3$, reflux, 3 h 30 (ii) HCl 37%, reflux, 1 h (78%); (c) (R = H) *m*-CPBA 90%, AcOH, 50 °C, 16 h (75%); (d) (R = CH_3) *m*-CPBA 90%, $CHCl_3$, rt, 4 h (79%).

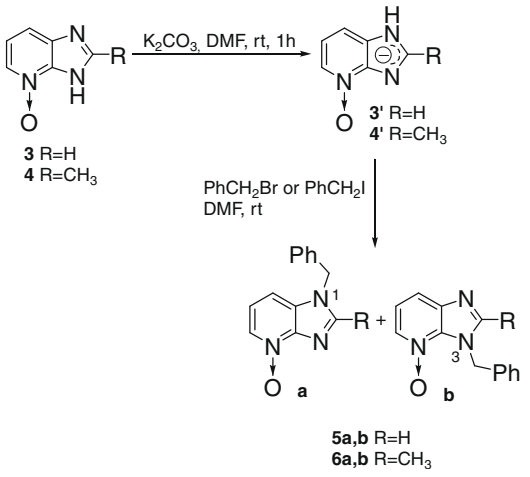

Scheme 2. N-Benzylation of 3*H*-imidazo[4,5-*b*]pyridine-4-oxide derivatives **3** and **4**.

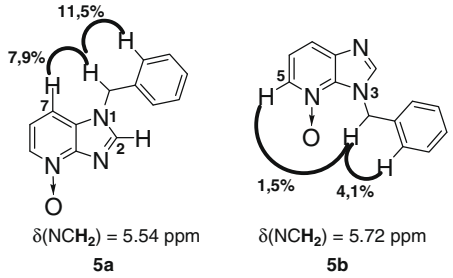

Figure 3. Establishment of the regioselectivity of N-benzylation of **5** by 1D nOe difference spectroscopy. ^{1}H NMR spectra were registered in DMSO-d_6.

Table 1
^{1}H NMR assignments of regioisomers **5a,b** and **6a,b** produced via Scheme 2

H	**5a**[a]	**5b**[a]	Δδ	**6a**[a]	**6b**[a]	Δδ
H-2	8.64 (s)	8.37 (s)		—	—	
CH_3	—	—		2.55 (s)	2.58 (s)	
H-5	8.20 (d)	8.39 (d)		8.12 (d)	8.17 (d)	
H-6	7.21 (dd)	7.17 (dd)		6.98 (dd)	7.03 (dd)	
H-7	7.60 (d)	8.32 (d)	**−0.72**	7.55 (d)	8.04 (d)	**−0.49**
N–CH_2	5.54 (s)	5.72 (s)	**−0.18**	5.53 (s)	5.67 (s)	**−0.14**

[a] ^{1}H spectra were recorded at 300 MHz in DMSO-d_6 at 23 °C. Chemical shifts are reported in part per million (ppm). In parentheses: multiplicity (coupling constants [*J*] in hertz are mentioned in Ref. 12).

Table 2
Results obtained for the N-benzylation of compounds **3** and **4** with benzyl bromide or benzyl iodide mentioned in Scheme 2

Entry	R	$PhCH_2X$	Time	*N*-1/*N*-3 ratio[a]	Yield[b] (%)
1	H	$PhCH_2Br$	20 h	(**5a**:**5b**) 60:40	86
2	H	$PhCH_2I$	4 h	(**5a**:**5b**) 70:30	84
3	CH_3	$PhCH_2Br$	20 h	(**6a**:**6b**) 40:60	60
4	CH_3	$PhCH_2I$	4 h	(**6a**:**6b**) 30:70	100

[a] *N*-1/*N*-3 ratios were determined after flash chromatography separation and ^{1}H NMR study.
[b] Total isolated yields.

Literature has shown that N-alkylation of imidazo[4,5-*b*]pyridine derivatives mainly led to *N*-3 regioisomer.[3,13] However, this NMR study has clearly confirmed that, whatever the alkylating agent we used and despite only a slight regioselectivity, 4-oxide **3** provided *N*-1 isomer as the major isomer under N-benzylation conditions (Table 2, entries 1 and 2).[7a,14] Meanwhile, opposite *N*-1/*N*-3 ratio was obtained when *C*-2-methylated 4-oxide **4** was treated under the same conditions (Table 2, entries 3 and 4). In both cases, benzyl iodide, used as alkylating agent, predictably provided more rapid reaction with more satisfactory *N*-1/*N*-3 ratios than benzyl bromide (Table 2, entries 2 and 4).

3. Computational methods

Calculations have been performed at the hybrid density functional B3LYP level[15] with GAUSSIAN 03 program.[16] The geometries were fully optimized without symmetry constraint. The standard all-electron 6-311+G(d) basis set was used for the Br, I, N, and O atoms while the basis set 6-311G(d, p) was used for the C and H atoms. Transition state (TS) geometries were approached by a linear-transit procedure, while optimizing all other degrees of freedom. Full TS searches were started from the geometries corresponding to maxima along the linear-transit curves. Each TS

displayed only one negative eigenvalue according to a non-ambiguous saddle point. The solvent corrections were taken into account by the Polarized Continuum Model (PCM)[17] implemented in the Gaussian program ($\varepsilon = 38$, DMF). All the energies were corrected of the basis set superposition error (BSSE) and the TS barriers have been corrected of the zero-point energy correction (ZPE). Atomic charges and atomic dipolar polarizations were calculated in the framework of the QTAIM theory[18] using the TopMoD package.[19] Ball-and-stick models of the TS structures have been displayed with the Molekel software.[20]

4. Density functional theory calculations

Starting from our experimental results, Density Functional Theory (DFT) calculations were next performed in order to provide a further understanding of the observed *N*-1/*N*-3 ratios and their relationship with alkylating agents. It seems likely that this slight *N*-1/*N*-3 regioselectivity variation may be due to non-bonded steric interactions governed by the geometries of the transition states (TS) involved in the N-alkylation mechanism. To determine the reaction pathway, S_N2-TS energies were compared to TS energies calculated for a hypothetical first step of dissociation of benzyl halide in a S_N1 mechanism ($PhCH_2^+ + X^-$). Actually, our calculations have clearly shown an energetic stabilization above 30 kcal/mol in favor of the S_N2 barriers in both gas and solvent phases.[21]

4.1. Regioisomers

The S_N2 regioisomers were optimized in both gas and solvent phases. All the relative energies are reported in Table 3. The main structural parameters of optimized structures are listed in Table 4. Whatever the alkylating agent we used, *N*-3 isomers were lower in energy than *N*-1 isomers in gas phase (Table 3). Conversely, *N*-1 isomers were found 3 kcal/mol lower in energy than *N*-3 isomers in solvent phase (Table 3). Thus, these results led us to conclude that a polar environment (DMF, $\varepsilon = 38$) was able to stabilize *N*-1 regioisomers better than *N*-3 ones. Tests of PCM calculations with modified parameters for the PCM environment (THF, $\varepsilon = 7.58$) led us to confirm these results since *N*-1 isomer **5a** (R = H) was found 1.8 kcal/mol more stable than *N*-3 isomer **5b** (R = H). Let us examine geometries of isomers in order to provide a further understanding of these results. In all cases, the plane of the benzyl group was perpendicularly staggered to imidazopyridine plane (Table 4). Consequently, steric hindrance between benzyl and imidazopyridine fragments appeared to be weak. Thus, because steric factors could not explain stability difference between *N*-1 and *N*-3 regioisomers, electronic charges have been calculated for each anion **3′** (R = H) and **4′** ($R = CH_3$) (Scheme 2) in gas phase and solvent. For the anion 3′, *N*-1 atomic charge value[18] was found quite similar to *N*-3 charge in gas phase (−0.90e). In contrast, the analysis of solvated anion **3′** revealed that the *N*-1 site was more polarized than *N*-3 site ones. Indeed, charges of *N*-1 and *N*-3 atoms are, respectively, determined to be −0.94e and −0.90e and local dipolar polarizations[17] were, respectively, calculated to be 0.45 a.u. and 0.40 a.u. These calculations have led to find out the preferred site (*N*-1 vs *N*-3) for a S_N2 mechanism in a polar solvent. Similar tendencies were found out in the case of anion **4′**. Moreover, the charge of the oxygen atom was found stronger for the ions in solvent phase (−0.70e) than in gas phase (−0.48e). So, a nucleophilic attack on *N*-3 site appeared electrostatically unfavorable in the solvated environment due to the strong repulsive interaction $O^- \cdots X^-$. All these electronic factors led us to conclude that nucleophilic attack was a slightly more favorable on *N*-1 site. Therefore, they allowed to easily grasp why the *N*-1 regioisomers were always more stable than *N*-3 ones in solvent phase. Nevertheless, observed *N*-1/*N*-3 ratios essentially depended on the relative stabilities of TS involved in the S_N2 process which has appeared to be the energetically preferred mechanism.

Table 3
Relative energies (kcal/mol) of products and transition states in gas and solvent phases, B3LYP optimized calculations

Transition states/products	$E_{gas+BSSE}$[b]	$E_{solv+BSSE}$[c]	ZPE[d]	$E_{sol+BSSE+ZPE}$[e]
TS-5-Bromide (R = H)				
*TS-**5a***	1.44	0.0	0.11 (0.12)	0.0
*TS-**5b***	0.0	0.34 (0.56)	0.0	0.23 (0.44)
TS-6-Bromide ($R = CH_3$)				
*TS-**6a***	2.32	0.38 (0.55)	0.0	0.23 (0.35)
*TS-**6a*** (2)[a]	2.45	0.95 (0.84)	0.06 (0.13)	0.86 (0.67)
*TS-**6b***	0.0	0.0	0.15 (0.20)	0.0
TS-5-Iodide (R = H)				
*TS-**5a***	2.17	0.0	0.0	0.0
*TS-**5b***	0.0	0.19	0.22	0.41
TS-6-Iodide ($R = CH_3$)				
*TS-**6a***	3.21	0.41	0.0	0.20
*TS-**6b***	0.0	0.0	0.22	0.0
Regioisomers				
5a	4.00	0.0		
5b	0.00	3.01 (3.18)		
6a	3.35	0.0		
6b	0.0	3.26 (3.20)		

[a] See Figure 4.
[b] Optimized energy in the gas phase.
[c] Single point and optimized (given in parentheses) solvent energy.
[d] Zero point energy correction in the gas phase. Values in parentheses correspond to the optimized geometries in the solvent phase.
[e] Relative electronic single point and optimized (given in parentheses) energies in the solvent phase including the BSSE and the ZPE corrections.

4.2. Transition state barriers

Relative energies of optimized S_N2 TS, in gas phase and solvent, are reported in Table 3. Single points were also calculated in solvent from the optimized gas phase geometries. They were found in reasonable agreement with the full optimized calculations. Main structural parameters of TS geometries are listed in Table 4. As displayed in Figure 4, *TS-**a*** structures (**5** or **6**) correspond to *N*-1-benzylated derivatives while *TS-**b*** structures (**5** or **6**) correspond to *N*-3-benzylated ones. As already observed for the final products (see previous section), *N*-3 barriers were widely stabilized in gas phase with respect to *N*-1 barriers (1.5–3.5 kcal/mol, see Table 3). However, it is worth noting that the relative gap between *N*-1 and *N*-3 barriers was apparently related to the nature of the group on *C*-2 position (H or CH_3). Indeed, the energetic gap between *TS-**5a*** (*N*-1 isomer, R = H) and *TS-**5b*** (*N*-3 isomer, R = H) was 1.44 kcal/mol, whereas the gap between *TS-**6a*** (*N*-1 isomer, $R = CH_3$) and *TS-**5b*** (*N*-3 isomer, $R = CH_3$) was greater than 2 kcal/mol (Table 3). Although these results in gas phase did not explain the experimental *N*-1/*N*-3 ratio variations, they confirmed that the gap *N*-1/*N*-3 was influenced by the steric hindrance of the methyl group on *C*-2 position. In contrast, the optimized calculations in solvent phase have appeared in fairly good agreement with experimentally observed ratios (Table 2) and have revealed a slight energetic difference (0.2–0.9 kcal/mol, Table 3) between *N*-1 and *N*-3 barriers. Indeed, *TS-**5a*** (*N*-1 isomer, R = H) was found slightly lower than *TS-**5b*** (*N*-3 isomer, R = H) in solvent. Conversely, in the presence of a methyl group on *C*-2 position (Fig. 4, bottom structures), *TS-**6b*** (*N*-3 isomer, $R = CH_3$) was found lower than *TS-**6a*** (*N*-1 isomer, $R = CH_3$). Consequently, *TS-**6a*** seemed to be less accessible than *TS-**6b*** in agreement with the observed experimental ratio **6a**:**6b** (Table 2, entries 3 and 4). Contrary to a hydrogen atom, the methyl group on *C*-2 position caused an additional steric interaction with the benzyl group. This can be understood by the geom-

Table 4
Structural parameters of TS and regioisomers optimized for both gas and solvent phases (given in parentheses) with respect to the numbering in Figure 4

	C^xN^{xa}	C^xX^b	N^4O	$C^xN^xC^{qa}$	$C^oC^xH^1H^2$	$C^oC^xN^xC2^a$
TS-Bromide						
TS-***5a***	2.219 (2.374)	2.515 (2.552)	1.289 (1.316)	124.9 (118.5)	175.5 (171.4)	0.0 (2.8)
TS-***5b***	2.146 (2.357)	2.615 (2.619)	1.299 (1.317)	130.8 (118.6)	176.6 (173.1)	85.6 (60.9)
TS-***6b***	2.220 (2.400)	2.541 (2.583)	1.290 (1.318)	115.2 (118.8)	178.5 (172.8)	4.1 (4.1)
TS-***6a***	2.154 (2.382)	2.629 (2.618)	1.302 (1.320)	128.5 (119.5)	175.6 (172.6)	85.7 (54.4)
TS-Iodide						
TS-***5a***	2.277	2.726	1.289	125.2	172.7	0.0
TS-***5b***	2.192	2.840	1.300	129.8	178.5	85.4
TS-***6b***	2.273	2.755	1.291	115.3	175.8	0.1
TS-***6a***	2.199	2.856	1.302	127.7	177.5	85.0
Products						
5a	1.478		1.302	126.0	120.5	38.1
5b	1.482		1.309	130.5	122.0	81.7
6a	1.469		1.304	126.2	120.0	74.6
6b	1.475		1.313	129.0	121.1	73.1

Distances are in Å and angles are in °.
[a] $N^x = N^1$ or N^3.
[b] X = Br or I.

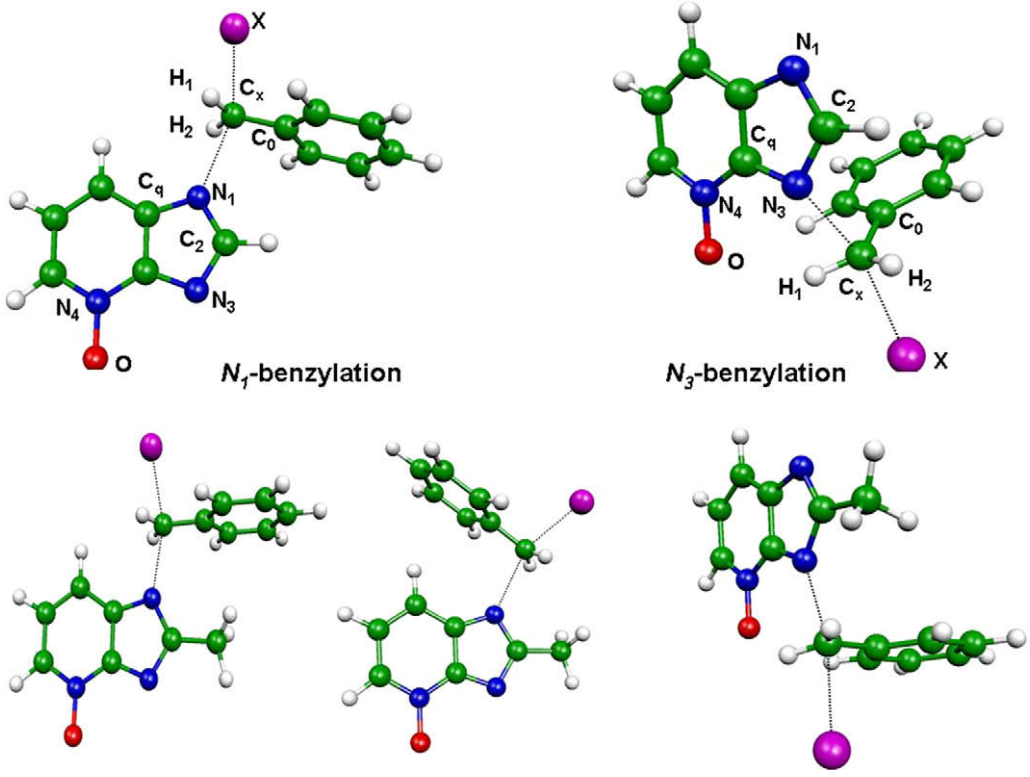

Figure 4. B3LYP optimized transition state structures for N-benzylation of imidazo[4,5-*b*]pyridine-4-oxide derivatives (ball-and-sticks models): *N1*-benzylation: *TS*-***5a*** (top,left), *TS*-***6a*** (bottom,left) and *TS*-***6a***(2) (bottom, middle). *N3*-benzylation: *TS*-***5b*** (top, right), *TS*-***6b*** (bottom, right).

etries of TS as displayed in Figure 5. As anticipated in S_N2 process, carbon C^x showed a typical strong sp2 character (Table 4). *TS*-***6a*** structure displayed a benzyl group directly orientated in front of the methyl (Fig. 5, left) whereas *TS*-***6b*** structure exhibited a staggered benzyl group with respect to the plane of the imidazopyridine moiety (Fig. 5, right). Thus, the methyl group induced a probable additional steric hindrance in the *N-1* transition state (*TS*-***6a*** structure) which was only partially balanced by the stabilizing solvent effects. Therefore, *TS*-***6b*** became slightly more stable than *TS*-***6a***. Another structure *TS*-**6a**(2) (Fig. 4, bottom middle) was also determined but, this transition state appeared to be destabilized since its energy was 0.3 kcal/mol higher than *TS*-**6a** one (Fig. 4, bottom left). This higher destabilization of *TS*-**6a**(2) could be probably explained by electrostatic repulsive effects between benzyl group and imidazopyridine moiety.

Thus, solvent effects strongly stabilized *N*-1 barrier (vs *N*-3 barrier) when a hydrogen atom is bonded to the *C*-2 position. On the other hand, in the presence of a methyl group on *C*-2 position, *N*-3 barrier remained lower than *N*-1 one in gas phase and solvent highlighting that, in this case, the regioselectivity of N-alkylation was mainly controlled by steric factor. So, our calculations have confirmed what literature has conveyed so far, that is, that regioselectivity in N-alkylation of azaheterocycle systems appeared essentially governed by 'steric approach control'.[21]

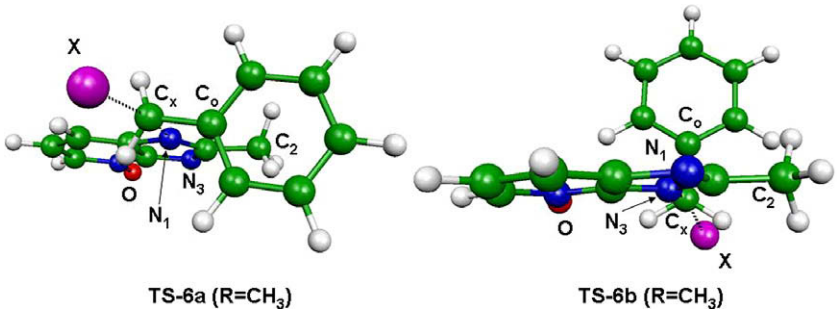

Figure 5. Comparative orientation of the benzyl plane in the *TS-**6a*** and *TS-**6b*** structures.

4.3. Alkylating agent effect

Both experimental and computational results have shown that the nature of benzyl halide slightly influenced *N*-1/*N*-3 ratios. Indeed, calculated relative energetic orders of the TS barriers in solvent were quite similar whatever the alkylating agent was used. However, optimized TS structures calculated with benzyl iodide (*TS-**5b*** structure) led to a more important steric hindrance between halide atom and the *N*-oxide group than with benzyl bromide. Consequently, the energetic gap between *TS-**5b*** and *TS-**5a*** has appeared slightly larger in the presence of iodide than in the presence of bromide. This probably explained that more satisfactory *N*-1/*N*-3 ratios were obtained with benzyl iodide (Table 2, entry 2). However, in the case of N-alkylation of derivative **4**, both steric effects induced either by the presence of a CH_3 group on *C*-2 position or by the use of a bulky iodide atom have a competitive influence on the structures *TS-**6a*** and TS-***6b***. So, the rationalization of the energetic gap between the latter structures is clearly more complex than the qualitative understanding previously given.

4.4. Concluding remarks

N-Benzylation of imidazo[4,5-*b*]pyridine-4-oxide derivatives substituted or not on *C*-2 position has been realized to afford, in each case, a mixture of *N*-1 and *N*-3 regioisomers. Both synthetic and theoretical studies have shown the following. (1) Calculations have determined that this nucleophilic substitution reaction occurred through a S_N2 pathway in solvent phase. (2) Experimental *N*-1/*N*-3 regioselectivities have been confirmed by DFT study. For each imidazo[4,5-*b*]pyridine-4-oxide derivatives, electronic factors (atomic charge and dipolar polarization) allowed concluding that nucleophilic attack was a slightly more favorable on *N*-1 site. But observed *N*-1/*N*-3 ratios essentially depended on the relative stabilities of TS involved in the S_N2 process in solvent. Our calculations have confirmed that regioselectivity in N-alkylation of azaheterocycles has appeared essentially governed by the 'steric approach control'. Indeed, the presence of a methyl group on *C*-2 position has induced additional steric interaction between the benzyl group and the CH_3 moiety. Therefore, in the case of 4-oxide **4**, *N*-3 regioisomer is the major one. Finally, syntheses of 1-substituted or 3-substituted imidazo[4,5-*b*]pyridin-7-one derivatives are in progress in our laboratory.

References and notes

1. (a) Chang, G. *FEBS Lett.* **2003**, *555*, 102–105; (b) Flügge, U. I.; Van Meer, G. *FEBS Lett.* **2006**, *580*, 997. and further articles of this special issue focused on ABC transporters.
2. Coombs, G. H. *Parasitol. Today* **1999**, *15*, 333–338.
3. Yutilov, Y. M. *Heterocycl. Chem.* **2005**, *89*, 159–270. and references therein.
4. Legraverend, M.; Grierson, D. S. *Bioorg. Med. Chem.* **2006**, *14*, 3987–4006.
5. Antonini, I.; Cristalli, G.; Franchetti, P.; Grifantini, M.; Martelli, S.; Petrelli, F. *J. Pharm. Sci.* **1984**, *73*, 367–369.
6. (a) Dubey, R. *Indian J. Chem., Sect. B* **1978**, *16*, 531; (b) Meravi, M. M.; Montazeri, N.; Rahmizadeh, M.; Bakavoli, M.; Ghassemzadeh, M. *J. Chem. Res. S* **2000**, *12*, 584–585.
7. (a) Itoh, T.; Ono, K.; Sugawara, T.; Mizuno, Y. *J. Heterocycl. Chem.* **1982**, *19*, 513–517; (b) Mizuno, Y.; Ikekawa, N.; Itoh, T.; Saito, K. *J. Org. Chem.* **1965**, *30*, 4066–4071.
8. Ochiai, E. *J. Org. Chem.* **1953**, *18*, 534–551.
9. *Synthesis of 2-methyl-3H-imidazo[4,5-b]pyridine-4-oxide* **4**: *m*-Chloroperbenzoic acid (90%, 5.690 g, 30 mmol) was added to a suspension of 2-methyl-3*H*-imidazo[4,5-*b*]pyridine **2** (1.587 g, 12 mmol) in chloroform (78 mL). The mixture was stirred for 4 h at room temperature. Evaporation of the solvent afforded a yellow powder which was loaded onto silica and was purified by column chromatography (CH_2Cl_2/acetone/MeOH = 7:1.5:1.5, R_f = 0.19) to give **4** (1.400 g, 79%) as a pale yellow solid. Mp 266–268 °C. ^{1}H NMR (300 MHz, DMSO-d_6): δ = 8.09 (d, ^3J(H,H) = 6.4 Hz, 1H, H-5), 7.50 (d, ^3J(H,H) = 8.1 Hz, 1H, H-7), 7.14 (dd, ^3J(H,H) = 6.4 and 8.1 Hz, 1H, H-6), 2.53 ppm (s, 3H, CH_3). HRMS (CI): *m/z*: calcd for $C_7H_8N_3O$: 150.0666, [M^++H]; found: 150.0667.
10. (a) Geen, G. R.; Kincey, P. M.; Spoors, P. G. *Tetrahedron Lett.* **2001**, *42*, 1781–1784; (b) Novak, J.; Linhart, I.; Dvarakova, H.; Kubelka, V. *Org. Lett.* **2003**, *5*, 637–639.
11. (a) Wenzel, T.; Seela, F. *Helv. Chim. Acta* **1996**, *79*, 169–178; (b) Geen, G. R.; Grinter, T. J.; Kincey, P. M.; Jarvest, R. L. *Tetrahedron* **1990**, *46*, 6903–6914.
12. *Typical experimental procedure for N-alkylation of imidazopyridine-4-oxide* **3** *and* **4**: K_2CO_3 (0.442 g, 3.2 mmol) was added under argon to a suspension of the imidazopyridine-4-oxide (2 mmol) in DMF (5 mL). After stirring at room temperature for 1 h, benzyl halide (2.4 mmol) was added. After overnight stirring, water was added and aqueous phase was extracted by AcOEt. The combined organic extracts were washed with water, dried (Na_2SO_4) and evaporated to give a red oil which was purified by column chromatography. In both cases, this general procedure afforded to a mixture of *N*-1/*N*-3 regioisomers. Regioisomer **5a** (CH_2Cl_2/MeOH = 95:5, R_f = 0.08, white powder, 71%). Mp 174–176 °C. ^{1}H NMR (300 MHz, DMSO-d_6, ppm): δ = 8.64 (s, 1H, H-2), 8.20 (d, ^3J(H,H) = 6.3 Hz, 1H, H-5), 7.60 (d, ^3J(H,H) = 8.3 Hz, 1H, H-7), 7.40–7.25 (m, 5H, Harom), 7.21 (dd, ^3J(H,H) = 6.3 and 8.3 Hz, 1H, H-6), 5.54 (s, 2H, CH_2). ^{13}C NMR (75 MHz, DMSO-d_6, ppm): δ = 147.5, 146.0, 136.8, 134.1, 131.2, 129.7, 129.2, 128.4, 120.0, 110.7, 49.4. HRMS (CI): *m/z*: calcd for $C_{13}H_{12}N_3O$: 226.0980, [M^++H]; found: 226.0977. Regioisomer **5b**: (CH_2Cl_2/MeOH = 95:5, R_f = 0.22, yellow powder, 17%). Mp 101–103 °C. ^{1}H NMR (300 MHz, DMSO-d_6, ppm): δ = 8.39 (d, ^3J(H,H) = 6.8 Hz, 1H, H-5), 8.37 (s, 1H, H-2), 8.32 (d, ^3J(H,H) = 7.7 Hz, 1H, H-7), 7.51–7.39 (m, 5H, H-arom), 7.17 (dd, ^3J(H,H) = 6.8 and 7.7 Hz, 1H, H-6), 5.72 (s, 2H, CH_2). ^{13}C NMR (75 MHz, DMSO-d_6, ppm): δ = 160.2, 146.3, 146.1, 133.0, 129.9, 129.5, 129.4, 128.9, 128.6, 112.0, 80.1. HRMS (EI): *m/z*: calcd for $C_{13}H_{11}N_3O$: 225.0902, [M^+]; found: 225.0903. Regioisomer **6a**: (CH_2Cl_2/MeOH = 90:10, R_f = 0.25, white powder, 30%). Mp 194–196 °C. ^{1}H NMR (300 MHz, DMSO-d_6, ppm): δ = 8.12 (d, ^3J(H,H) = 6.4 Hz, 1H, H-5), 7.55 (d, ^3J(H,H) = 8.3 Hz, 1H, H-7), 7.38–7.27 (m, 3H, H-arom), 7.20–6.97 (m, 3H, H-6, 2 × H-arom), 5.53 (s, 2H, CH_2), 2.55 (s, 3H, CH_3). ^{13}C NMR (75 MHz, DMSO-d_6, ppm): δ = 171.5, 149.9, 148.3, 134.0, 130.7, 130.3, 129.5, 127.6, 126.6, 112.2, 80.7, 19.6. HRMS (EI): *m/z*: calcd for $C_{14}H_{13}N_3O$: 239.1059, [M^+]; found: 239.1058. Regioisomer **6b**: (CH_2Cl_2/MeOH = 90:10, R_f = 0.62, white powder, 70%). Mp 100–102 °C; ^{1}H NMR (300 MHz, DMSO-d_6, ppm): δ = 8.18 (d, ^3J(H,H) = 6.8 Hz, 1H, H-5), 8.05 (d, ^3J(H,H) = 7.7 Hz, 1H, H-7), 7.50–7.41 (m, 5H, H-arom), 7.03 (dd, ^3J(H,H) = 6.8 and 7.7 Hz, 1H, H-6), 5.67 (s, 2H, CH_2), 2.58 ppm (s, 3H, CH_3); ^{13}C NMR (75 MHz, DMSO-d_6, ppm): δ = 162.9, 154.7, 146.5, 133.7, 132.8, 129.8, 128.7, 127.7, 119.2, 109.7, 47.9, 14.7. HRMS (EI): *m/z*: calcd for $C_{14}H_{13}N_3O$: 239.1059, [M^+]; found: 239.1055.
13. (a) Chang, L. C. W.; von Frijtag Drabbe Künzel, J. K.; Mulder-Krieger, T.; Westerhout, J.; Spangenberg, T.; Brussee, J.; IJzerman, A. P. *J. Med. Chem.* **2007**, *50*, 828–834; (b) Khanna, I. K.; Weier, R. M.; Lentz, K. T.; Swenton, L.; Lankin, D. C. *J. Org. Chem.* **1995**, *60*, 960–965; (c) Franchetti, P.; Cappellacci, L.; Grifantini, M.; Messini, L.; Sheikha, G. A.; Loi, A. G.; Tramontano, E.; De Montis, A.; Spiga, M. G.; La Colla, P. *J. Med. Chem.* **1994**, *37*, 3534–3541; (d) Cristalli, G.; Franchetti, P.; Grifantini, M.; Vittori, S.; Bordoni, T.; Geroni, C. *J. Med. Chem.* **1987**, *30*, 1686–1688.
14. Itoh, T.; Sugawara, T.; Mizuno, Y. *Nucleosides Nucleotides* **1982**, *2*, 179–190.

15. (a) Lee, C.; Yang, W.; Parr, R. G.. *Phys. Rev. B* **1988**, *37*, 785–789; (b) Becke, A. D. *J. Chem. Phys.* **1993**, *98*, 5648–5652.
16. Frisch, M. J.; Trucks, G. W.; Schlegel, H. B.; Scuseria, G. E.; Robb, M. A.; Cheeseman, J. R.; Montgomery Jr., J. A.; Vreven, T.; Kudin, K. N.; Burant, J. C.; Millam, J. M.; Iyengar, S. S.; Tomasi, J.; Barone, V.; Mennucci, B.; Cossi, M.; Scalmani, G.; Rega, N.; Petersson, G. A.; Nakatsuji, H.; Hada, M.; Ehara, M.; Toyota, K.; Fukuda, R.; Hasegawa, J.; Ishida, M.; Nakajima, T.; Honda, Y.; Kitao, O.; Nakai, H.; Klene, M.; Li, X.; Knox, J. E.; Hratchian, H. P.; Cross, J. B.; Bakken, V.; Adamo, C.; Jaramillo, J.; Gomperts, R.; Stratmann, R. E.; Yazyev, O.; Austin, A. J.; Cammi, R.; Pomelli, C.; Ochterski, J. W.; Ayala, P. Y.; Morokuma, K.; Voth, G. A.; Salvador, P.; Dannenberg, J. J.; Zakrzewski, V. G.; Dapprich, S.; Daniels, A. D.; Strain, M. C.; Farkas, O.; Malick, D. K.; Rabuck, A. D.; Raghavachari, K.; Foresman, J. B.; Ortiz, J. V.; Cui, Q.; Baboul, A. G.; Clifford, S.; Cioslowski, J.; Stefanov, B. B.; Liu, G.; Liashenko, A.; Piskorz, P.; Komaromi, I.; Martin, R. L.; Fox, D. J.; Keith, T.; Al-Laham, M. A.; Peng, C. Y.; Nanayakkara, A.; Challacombe, M.; Gill, P. M. W.; Johnson, B.; Chen, W.; Wong, M. W.; Gonzalez, C. and Pople, J. A., GAUSSIAN 03, Revision D.01 Gaussian, Wallingford CT, 2004.
17. (a) Cossi, M.; Barone, V.; Cammi, R.; Tomasi, J. *Chem. Phys. Lett.* **1996**, *255*, 327–335; (b) Boys, S. F.; Bernardi, F. *Mol. Phys.* **1970**, *19*, 553–566.
18. Bader, R. F. W. In *Atoms in Molecules: A Quantum Theory*; Oxford Univ. Press: Oxford, 1990.
19. (a) Noury, S.; Krokidis, X.; Fuster, F.; Silvi, B. *Comput. Chem.* **1999**, *23*, 597–604; (b) Pilme, J.; Piquemal, J.-P. *J. Comput. Chem.* **2008**, *29*, 1440–1449.
20. Flukiner, P.; Luthi, H. P.; Portman, S.; Weber, J. *Molekel*; Swiss Center for Scientific Computing: Switzerland, 2000–2002.
21. Haque, M. R.; Rasmussen, M. *Tetrahedron* **1994**, *50*, 5535–5554.